

Biasing in the Galaxy Distribution

C. Benoist

LAEC, CNRS, Observatoire de Paris-Meudon, 5 Pl. J. Janssen, 92195 Meudon Cedex,
France.

benoist@gin.obspm.fr

S. Maurogordato

LAEC, CNRS, Observatoire de Paris-Meudon, 5 Pl. J. Janssen, 92195 Meudon Cedex,
France.

maurogor@gin.obspm.fr

L.N. da Costa¹

European Southern Observatory, Karl-Schwarzschild-Str.2, D-85748 Garching bei
München, Germany.

ldacosta@eso.org

A. Cappi

Osservatorio Astronomico di Bologna, via Zamboni 33, I-40126, Bologna, Italy.

cappi@astbo3.bo.astro.it

and

R. Schaeffer

Service de Physique Théorique, CEN-Saclay, F-91191, Gif-sur-Yvette Cedex, France.

schaeffer@amoco.saclay.cea.fr

Received _____; accepted _____

¹and Departamento de Astronomia CNPq/Observatório Nacional, rua General José
Cristino 77, Rio de Janeiro, R.J. 20921 Brazil.

ABSTRACT

We investigate the variation of galaxy clustering with luminosity using the recently completed SSRS2 sample. Clustering measurements based on the two-point correlation function and the variance of counts in cells reveal a strong dependence of clustering on luminosity for galaxies brighter than L_* , while no significant variation is detected for fainter galaxies. We derive a relative bias versus magnitude relation which can be compared with theoretical predictions. Existing models of galaxy formation cannot adequately reproduce the simultaneous steep rise of biasing at high luminosities and the plateau at the low-luminosity end. Improved modeling of halo-galaxy relation, and larger samples including low luminosities galaxies are required to draw more definitive conclusions.

Subject headings: cosmology, galaxies: clustering, large-scale structure of the universe

1. Introduction

Redshift surveys of galaxies have provided over the years a wealth of information that has greatly contributed to our understanding of the way galaxies are distributed in space. However, these observational results on galaxy clustering are not easily used to constrain theoretical models because of our poor understanding of the relation between galaxy and mass distributions.

Although until recently the main emphasis of redshift surveys has been on the study of large-scale structure, several attempts have been made to understand the dependence of galaxy clustering on their internal properties such as luminosity, morphology, and surface brightness. An understanding of the relative bias between different galaxy populations is essential for constraining models of galaxy formation. Most of these studies were based on the first generation of redshift surveys like CfA1 (Huchra et al. 1983) and SSRS (Southern Sky Redshift Survey) (da Costa et al. 1988) which were not suitable for this kind of analysis because of the small volume surveyed and of the relative small number of galaxies in the samples.

Not surprisingly the results have so far been rather controversial, with some authors claiming evidence of luminosity segregation in the data (see for instance Hamilton 1988, Davis et al. 1988, Börner, Mo and Zhou 1989, Dominguez-Tenreiro & Martinez 1989, Börner, Deng and Xia 1989, Maurogordato & Lachièze-Rey 1991, Maurogordato, Schaeffer and da Costa 1992) while others arguing against it (as Phillipps & Shanks 1987, Thuan et al. 1987, Alimi et al. 1988, Eder et al. 1989, Haynes & Giovanelli 1989, Bingelli et al. 1990, Thuan et al. 1991, Hasegawa & Umemura 1993). While the dependence of clustering on morphology is well established (Davis & Geller 1976, Santiago & da Costa 1990, Börner & Mo 1990, Mo et al. 1992, Iovino et al. 1993, Dominguez-Tenreiro et al. 1994), the dependence on luminosity is still a matter of debate.

Recently, a new generation of redshift surveys has been completed calling for a new examination of the problem. Recent estimates of the galaxy power spectrum from the CfA2 (Park et al. 1994), and of the correlation function for Stromlo-APM (Loveday et al. 1995) redshift surveys seem to show that some luminosity segregation does exist, but a consensus has still not been reached over the range of magnitudes at which the effect occurs. In this paper we will analyze in detail the dependence on luminosity of the correlation function and of the variance of counts in cells using the recently completed SSRS2. The combination of dense sampling, large sky coverage and a large number of galaxies allows us to define various subsamples to investigate separately different effects that may have a bearing on our conclusions. In section 2 we describe the sample and the corrections applied to the data. In section 3 we discuss the different statistics applied in our analysis, investigate the dependence of clustering on luminosity and compare our results to those of previous work. In section 4 we discuss the implications of our results on models of galaxy formation. A brief summary of our main conclusions is presented in section 5.

2. The data

In the analysis presented below we use the SSRS2 (da Costa et al. 1994), a magnitude-limited redshift survey centered on the south galactic pole. It includes ~ 3600 galaxies and covers 1.13 sr, delimited by $-40^\circ < \delta < -2.5^\circ$ and $b < -40^\circ$, complete up to limiting magnitude $m_{B(0)} = 15.5$. Radial velocities have been corrected to the Local Group rest frame (Yahil et al. 1977).

Since all galaxies in the SSRS2 have been assigned morphological types following the ESO-Uppsala classification system (T), we have adopted a morphological-dependent K-correction, $K(z, T)$, to compute the absolute magnitude of a galaxy according to the expression

$$M = m - 25 - 5 \log D_L - K(z, T) \quad (1)$$

where D_L is the luminosity distance for standard Friedman models:

$$D_L = \frac{c}{H_0} \frac{1}{q_0^2} [1 - q_0 + q_0 z + (q_0 - 1) \sqrt{2q_0 z + 1}] \quad (2)$$

In the following analysis we have adopted $H_0 = 100$, $q_0 = 0.5$. We have divided the sample in four morphological classes and applied for each class the K-correction following Efstathiou, Ellis & Peterson (1988):

E/SO	$-5 \leq T \leq 0$	$K = 4.14z$
Sa, Sb, Sbc	$1 \leq T \leq 4$	$K = 2.90z$
Sc, Scd	$5 \leq T \leq 6$	$K = 2.25z$
Sdm	$7 < T$	$K = 1.59z$

Volume-limited samples were defined adopting a “minimum distance” criterium by taking galaxies within a depth corresponding to the smallest D_L among those calculated for the different morphological classes, which corresponds in our case to the depth of the early-type galaxies. Luminosity distances were then converted into comoving distances.

3. Analysis

3.1. Statistics

We examine the clustering properties of galaxies using the two-point correlation function $\xi(s)$ and the J_3 integral, computed by counting the number of galaxy pairs

in shells, and the variance σ^2 of galaxy counts in excess of Poisson derived from count probabilities in randomly placed spheres.

The two-point correlation function in redshift-space was computed using the following estimator (Hamilton, 1993):

$$1 + \xi(s) = \frac{DD(s)RR(s)}{DR^2(s)} \quad (3)$$

where DD is the number of the galaxy-galaxy pairs, DR is the number of galaxy-random point pairs and RR is the number of pairs in the random catalog with a separation in the interval s and $s + ds$. This estimator is less sensitive to uncertainties of the mean density, which is a second order effect in contrast to the previously defined estimator (Davis & Peebles 1983). Since we only consider samples limited both in distance and in absolute magnitude we adopt uniform weighting in the pair-counts defined above. From these pair counts in shells, we have also computed the so-called J_3 integral (Peebles 1980)

$$J_3(s) = \int_0^s u^2 \xi(u) du \quad (4)$$

which represents (up to a factor of 4π) the mean number of excess galaxies around each galaxy within a distance s . We use this statistic in section 4 to derive the relative bias between different luminosity classes.

Another way to characterize the clustering properties of galaxies consists in calculating the probability $P(N, l)$ of finding N galaxies in spherical cells of radii l placed at random. In this procedure, the spheres crossing the edges of the samples are rejected. The number of trials is chosen in order to have small statistical errors at scales larger than $2h^{-1}$ Mpc (see the discussion in Appendix B of Maurogordato, Schaeffer, da Costa, 1992). This leads in our case to 10^4 to 10^6 trials, from the shallower to the deeper sample. We have derived the variance of these counts in cells which can be expressed as

$$\langle (N - \bar{N})^2 \rangle = \bar{N}(1 + N_c), \quad (5)$$

where n is the mean density of the sample, $\bar{N} = nV$ is the mean number of objects, and $N_c = n^2V^2\sigma^2$ is the mean number of objects in excess of random inside a sphere of volume V . The variance can be related to the volume-averaged correlation function

$$\sigma^2(s) \equiv \bar{\xi}(s) = \frac{1}{V^2} \int_V \xi(s) d^3s_1 d^3s_2 \quad (6)$$

In the power law approximation, $\xi(s) = (s_0/s)^\gamma$, this can be expressed as

$$J_3(s)/V = \frac{1}{(1 - \gamma/3)} \xi(s) \quad (7)$$

$$\sigma^2(s) = \frac{2^{-\gamma}}{(1 - \gamma/3)(1 - \gamma/4)(1 - \gamma/6)} \xi(s) \quad (8)$$

In this case $J_3(s)/V$ and $\sigma^2(s)$ are related by a multiplicative factor depending weakly on γ in the range of interest (0.8 for $\gamma = 1$, 0.75 for $\gamma = 2$). Below we will compare the results obtained from both methods to test our conclusions.

3.2. Volume and Luminosity limited Samples

From the SSRS2 we have extracted nine volume and luminosity limited subsamples with their absolute magnitude limit separated by 0.5^m , ranging in depth from 30 to $168 h^{-1}$ Mpc . The characteristics of these samples are given in Table 1 where we list: in column (1) sample identification; in column (2) the depth as defined in the previous section; in column (3) the corresponding faint absolute magnitude limit of the sample; in column (4) the number of galaxies in the sample; in column (5) the mean density of galaxies.

EDITOR: PLACE TABLE 1 HERE.

For each of these samples we have computed $\xi(s)$, $J_3(s)$ and $\sigma^2(s)$, and derived power-law fits to $\xi(s)$ in the range of separations where it is a good approximation (this

range is not the same for all the samples). The correlation parameters derived from these fits are listed in columns (6) and (7) of Table 1 where we give the correlation length s_0 and slope γ for a two-parameter fit in the separation range range given in column (9). For comparison we list in column (8) the correlation length s'_0 obtained assuming a fixed slope $\gamma = 1.7$. In column (10) we give the value of the variance in $8h^{-1}$ Mpc spheres, σ_8^2 as derived from the analysis of counts in cells. Finally, in column (11), we list the ratio L/E of late type over early type galaxies.

EDITOR: PLACE FIGURE 1 HERE.

Figure 1 shows $\xi(s)$, $J_3(s)$ and $\sigma^2(s)$ for the samples given in Table 1. The error bars correspond to the rms value as measured for 15 bootstrap re-samplings of each sample. In the case of the less dense samples, errors on the various statistics on small scales can be very large. Therefore, here and in the following graphs, error bars for these samples are shown as dotted and dashed lines in order to avoid over-crowding of the plots. While we do not find any systematic variation of the slope with depth (table 1), the correlation length varies significantly over the range of depths considered especially for the deepest samples containing the brightest galaxies. The observed variation is consistent to that shown in Davis et al. (1988) but now probing much larger depths for a given absolute magnitude limit. The same trend for an apparent increase in the clustering strength with depth is seen in the number of neighbors $J_3(s)$ and in the variance computed from counts-in-cells. This variation is quantified by σ_8^2 listed in table 1.

A key question is whether the observed variation reflects the intrinsic nature of the galaxy distribution (e.g. Baryshev et al. 1995 and references therein), simply sampling variations or genuine luminosity segregation, since in deeper samples the fraction of intrinsically luminous galaxies increases. The discussion is particularly problematic since

comparison of the amplitude of the correlation function as determined from different volumes may be affected by sampling variations which can arise because different structures are probed for different volume-limited samples. This could induce fluctuations in the mean density of the sample or variations in redshift distortions as the sample probes different virialized systems and samples different regions of large-scale peculiar velocity field. Still another effect that could be introduced by redshift distortions would be if more luminous galaxies were found preferentially within virialized systems, as a product of mergers for instance. In this case, redshift distortions could also affect the comparison of samples even within the same volume.

Ideally, to prove the existence of luminosity segregation one should compare the clustering properties of different luminosity classes within the same volume and in real space. Recently, this has become partially possible thanks to the large number of galaxies in complete dense surveys like the SSRS2. The large number of galaxies allows the sample to be divided in different ways to discriminate between the various effects discussed above. This can be achieved by comparing the clustering properties of galaxies of different luminosity classes within the same volume and the clustering of galaxies in the same luminosity class but in different volumes. Although dividing the sample in this fashion reduces the number of galaxies in each subsample, thus increasing the uncertainties of the various statistics, it makes it possible to distinguish the contribution that different effects may have on the $\xi(s)$ derived from volume-limited samples like those used in figure 1.

EDITOR: PLACE FIGURE 2 HERE.

In figure 2 we show $\xi(s)$ for three different volumes ($D = 38h^{-1}$ Mpc, $D = 60h^{-1}$ Mpc, $D = 91h^{-1}$ Mpc). For each volume we have compared the clustering properties of galaxies in contiguous magnitude bins 1^m wide. Unfortunately, the sample is not large

enough to allow this comparison to be made over a wider range of luminosity classes since we are constrained by the apparent magnitude limit of the sample and by the number of galaxies in each class. In our case we are limited to only two adjacent magnitude bins given in Table 2. The depth was chosen to correspond to the maximum distance at which the faintest galaxies considered are visible. Dividing the sample in this way allows us to test for luminosity segregation in a way that is insensitive to sampling variations.

EDITOR: PLACE TABLE 2 HERE.

We note from figure 2 that faint galaxies do not exhibit any significant relative bias. While there is some slight indication of segregation for galaxies in the range $-20.5 \leq M \leq -19.5$ relative to galaxies in the magnitude interval $-19.5 \leq M \leq -18.5$ (panel b), it is only in the largest volume considered that we find a significant effect. This result implies that galaxies brighter than -20.5 are significantly more clustered than those in the range $-20.5 < M < -19.5$. Based on these results we infer that the onset of this segregation occurs roughly at $M = -19.5$, close to L_* .

EDITOR: PLACE FIGURE 3 HERE.

In order to examine the importance of sampling variations we show in figure 3 measurements of $\xi(s)$ for galaxies in the same luminosity class in three different volumes of increasing depth. The characteristics of these subsamples are also summarized in Table 2. From the plot we find that the clustering of faint galaxies seen only in relatively nearby samples is not stable which reflects strong fluctuations in the mean density. This is clearly seen in panel (a) where we show $\xi(s)$ for galaxies in the luminosity range $-19.5 \leq M \leq -18.5$ in volumes ranging from 38 to 60 h^{-1} Mpc in depth as indicated in the figure. For the faintest range considered the volumes are relatively small and one finds

some variation in the correlation function at large separations with the amplitude of $\xi(s)$ computed in the $60 h^{-1}$ Mpc volume being significantly larger for $s > 6 h^{-1}$ Mpc . This is not surprising since the size of the samples are comparable to the scale of inhomogeneities leading to important fluctuations in the mean density. This is not the case for the brighter subsamples probing volumes with depths $D > 60 h^{-1}$ Mpc . In fact, although one can see in figure 1 (a) an increase in the amplitude of the correlation function between, for instance, samples D38 and D60, no significant luminosity segregation is detected when comparing the $\xi(s)$ for different luminosity classes within the same volume. Instead $\xi(s)$ is seen to vary significantly with the depth of the volume considered.

By contrast, for galaxies brighter than $M = -19.5$, shown in panels (b) and (c) there is no evidence for variations in the correlation strength with the depth of the sample. This suggests that sampling variations affect our results only for samples that probe small volumes of space. This conclusion is confirmed by the fact that the ratio of $\xi(s)$ for galaxies in the D91 subsample and for galaxies in the sample D138 is consistent with the ratio of $\xi(s)$ for the same luminosity classes within the same volume. This indicates that luminosity segregation is responsible for the increase in the amplitude of $\xi(s)$ between sample D91 and D138 seen in Figure 1. We assume that the same is valid for galaxies brighter than $M = -21$, although we cannot verify this claim because the number of such bright galaxies rapidly decreases for smaller volumes. Nevertheless,

we have checked that the mean density within this sample, calculated in shells of different depths, does not show any systematical variation. In particular, no drop of the density with depth has been detected. Therefore the clustering properties of the very bright galaxies previously shown are not a spurious effect due to an hypothetical incompleteness. The properties of the subsample D168 are examined in detail in a forthcoming paper (Cappi et al. 1996).

Based on the previous discussion we conclude that the variation of the amplitude of the correlation function observed in Figure 1 has two contributions. The first due to sampling fluctuations which affects primarily the clustering of faint galaxies probing small volumes. This affects samples roughly to D74 or galaxies fainter than $M = -19$. The second effect is consistent with the interpretation that the clustering of galaxies depends on luminosity. In the discussion below, we use the correlation function of volume-limited samples including all galaxies brighter than a limiting value to derive the relative bias of galaxies as a function of luminosity. We do that because, although useful to investigate the onset of the segregation, comparison of galaxies in magnitude bins are not suitable for comparison with theoretical predictions.

3.3. Redshift Distortion and Morphology Effects

As different structures are probed by the samples used in figure 1, variations in the amplitude of the correlation could also be induced by redshift distortions. On small scales, virialized systems tend to lower the correlation amplitude, while on intermediate scales streaming motions enhance the correlation amplitude, when measured in redshift space (Kaiser 1987). However, as da Costa et al. (1995) have shown that redshift distortions are relatively weak within the volume surveyed by the SSRS2, we do not expect a strong impact on the statistics. Nevertheless, in order to quantify this effect, we have checked the behavior of the correlation function in real space on the previously tested samples. We have verified that the trend with luminosity is the same, and that the amplification factor between the various samples is quantitatively the same in real space as in redshift space. This shows that redshift space distortion are not responsible for the luminosity biasing evidenced by SSRS2 data.

We note that our results cannot be due to a morphology-luminosity relation since

Marzke et al. (1994) and da Costa et al. (1995) have shown that the luminosity functions for different morphological types are similar, except for irregulars. Moreover, we have verified that the morphological composition of our volume-limited samples is independent of the luminosity class adopted (Table 1, column (11)).

3.4. Comparison with previous results

The above results give further support to conclusions reached by Hamilton (1988), Davis et al. (1988) and Lachièze-Rey, da Costa and Maurogordato (1992) from their analyses of the CfA1 and SSRS redshift surveys, with significantly better statistics and extending the range of magnitudes over which the effect can be studied. First, both sampling effects and stronger clustering of more luminous galaxies are responsible for the variation of the correlation length with the depth of the sample. Sampling effects are important for the smaller volumes and are difficult to disentangle from luminosity effects below $M \sim -19$. However, luminosity segregation at the low-luminosity end, if present at all, should be small, as figure 2 shows no evidence for a variation of the clustering amplitude of galaxies in the magnitude interval $-18.5 \leq M \leq -17.5$ relative to those in the interval $-19.5 \leq M \leq -18.5$ within the volume of depth $30h^{-1}$ Mpc . Second, for brighter galaxies, probing larger volumes, sampling effects are not important and for a given luminosity limit there is no significant variation of the correlation amplitude with depth. On the other hand, comparison of different luminosity classes within the same volume shows robust evidence for a relative increase in the clustering strength as a function of the luminosity. The relative amplitude is the same as that deduced from considering galaxies in the magnitude bins in the same volume. Third, the values of the relative bias when comparing the brightest galaxies in the sample to galaxies fainter than L_* are in good agreement with the values obtained by Hamilton (1988) from the CfA1.

Signatures of luminosity segregation have also been detected by Park et al. (1994) from their power spectrum analysis of volume-limited subsamples drawn from CfA2. In particular, the amplification factor of ~ 1.4 between their subsamples at $101h^{-1}$ Mpc, $M \leq -19.7$ and $130h^{-1}$ Mpc, $M \leq -20.3$ is consistent with our findings, However, their comparison of the power spectrum from bright/faint galaxies in volume-limited samples is not easily compared to our results as they use different magnitude bins.

Evidence for luminosity-dependence of clustering have also been detected by Loveday et al. (1995) from a recent analysis of the correlation function on the Stromlo–APM redshift survey. Their conclusions differ from our findings as they show that while galaxies brighter than L_* ($-20 \leq M \leq -19$) are more clustered than fainter ones ($-19 \leq M \leq -15$), there is no evidence for stronger clustering of galaxies with $L > L_*$ ($-22 \leq M \leq -20$). The reasons for these differences are at the present unclear.

4. Bias and Comparison to Models

In order to quantify the dependence of the clustering strength on luminosity we define the relative bias b/b_* of galaxies brighter than M towards galaxies brighter than M_* (~ -19.5) as a function of scale s :

$$\frac{b}{b_*}(s) = \sqrt{\frac{\xi(s)}{\xi_*(s)}} \quad (9)$$

We have adopted the following notation for the various statistics applied: no subscript refers to galaxies brighter than M , and $*$ subscript refers to galaxies brighter than M_* .

On those scales where the correlation function is well fitted by a power law, $J_3(s)/V$ and $\sigma^2(s)$ are proportional to $\xi(s)$, and therefore the ratio $b/b_*(s)$ can alternatively be expressed in terms of $J_3(s)$ or of $\sigma^2(s)$ as

$$\frac{b}{b_*}(s) = \sqrt{\frac{J_3(s)}{J_3^*(s)}} \quad (10)$$

$$\frac{b}{b_*}(s) = \sqrt{\frac{\sigma^2(s)}{\sigma_*^2(s)}} \quad (11)$$

It is more convenient to work with expression (10) and (11) rather than with expression (9) as $J_3(s)$ or $\sigma^2(s)$, which are integrated statistics, make possible the derivation of smoother ratios.

As mentioned above, while the use of magnitude bins is useful to detect and to determine the onset of luminosity segregation, for comparison with theoretical predictions it is more convenient to use volume and absolute magnitude limited samples like those of Table 1. Results relative to $M > -19.0$ should be considered with caution before further interpretation, as sampling effects have been shown to be important for the smaller samples.

EDITOR: PLACE FIGURE 4 HERE.

The ratio b/b_* as a function of scale is presented in figure 4 as derived from ratios of $J_3(s)$ (panel a) and $\sigma^2(s)$ (panel b). It is worth noting that the ratio is roughly constant in the interval $2 < s < 13h^{-1}$ Mpc for the subsamples considered, indicating that the relative bias is independent of scale, which makes it possible to define a mean linear biasing factor, which varies from 0.8 for the faintest sample ($M \leq -19$) to 2 for the brightest sample ($M \leq -21.0$).

The variation of the linear bias with luminosity is shown in figure 5, where we show for comparison the same curve obtained by Hamilton (1988) from the CfA1 survey. As can be seen there is a remarkable agreement at the bright end between these estimates based on samples probing different structures. It is important to emphasize that the SSRS2 sample

is not affected by uncertainties in the Virgo infall which has been used as an argument against Hamilton’s interpretation of his results based on CfA1 data.

EDITOR: PLACE FIGURE 5 HERE.

Luminosity biasing is expected to be present in the galaxy distribution according to most scenarios of galaxy formation. In the standard scheme of biased galaxy formation (Bardeen et al. 1986), galaxies are assumed to form from peaks above some global threshold in the primordial smoothed density field. This implies a dependence of the correlation function on the threshold which can be converted into a dependence on luminosity once a luminosity or circular velocity-peak relation is determined. Direct evidence that the amplitude of the correlation function increases with the circular velocity of the halos has been found both in numerical simulations of hierarchical clustering (White et al 1987) and in an extension of the Press-Schechter formalism (Mo and White 1995). Comparing these predictions to our data requires the knowledge of the relation between halos and galaxies. We have compared our results to these predictions by expressing circular velocities in terms of luminosities by the Tully-Fisher and Faber-Jackson relations (White, Tully and Davis 1988 and Valls-Gabaud, Alimi and Blanchard 1989). We have normalized the results for all the samples tested to the sample with galaxies brighter than L^* . As shown in figure 5, even in the case of low normalization ($\sigma_8=0.5$), it is difficult to mimic the steep increase of clustering present in the data at $L > L^*$. Moreover, all models exhibit a clear luminosity dependence also at low luminosities which is difficult to test from the data as low-luminosity samples are also nearby and have been shown to be sensitive to sampling fluctuations. Still, as discussed before, the lack of luminosity segregation inside single volume-limited nearby samples as shown in figure 3 tends to indicate that a *strong* segregation at the low-luminosity end is quite unlikely. Note that this comparison is only suggestive as a one-to-one correspondence has been assigned to galaxy-halo pairs. More

elaborated modeling of the properties of galaxies and halos (Kauffmann, 1995) will allow a more precise comparison of luminosity biasing to the prediction of models for *galaxies*.

An alternative view on the origin of biasing can be obtained from a description of the density field behavior at scales where it is strongly non-linear (Schaeffer 1984, 1985, Balian & Schaeffer 1989). This approach yields an analytic description of the matter fluctuations, based on an assumption about the scaling of the many-body matter correlation functions inspired by dynamical considerations (Peebles 1980, Balian & Schaeffer 1989). These models imply a bias in the distribution of high density spots. However, this bias is not acquired at the birth of the over-densities as a result of the initial Gaussian conditions, and then frozen. It is the result (Schaeffer 1985, 1987) of the non-linear evolution, and is determined once the density fluctuations are known. A specific calculation (Bernardeau & Schaeffer 1992) shows that for all models with the above scaling, the bias depends only on the internal properties of the objects whose correlations are considered. More specifically it increases as a function of a unique parameter, closely related to the gravitational potential, and therefore increases with luminosity. This analytical model gives explicitly the asymptotic behavior for the brightest galaxies: b/b^* is nearly proportional to L/L^* . It is very successful in reproducing the steep increase of the correlation function for bright galaxies $L > L^*$ but it predicts a strong luminosity segregation at faint luminosities which is very difficult to reconcile with the data (figure 5). Larger samples of galaxies going to fainter magnitudes are therefore necessary to test the models at the low-luminosity end.

5. Summary

Using the recently completely SSRS2 redshift survey we have investigated the dependence of the clustering properties of galaxies on luminosity. The SSRS2 sample is particularly suitable for this study because of the large number of galaxies, the paucity of

rich clusters within the volume and the small amplitude of redshift distortions induced by peculiar motions both at small and large scales. Analysis of volume-limited samples using both the two-point correlation function and the variance of counts in cells indicate that galaxy clustering depends on luminosity. The effect is small for faint galaxies but increases dramatically for galaxies brighter than L_* . The correlation length varies from about $5 h^{-1}$ Mpc, for the faintest galaxies up to $8 h^{-1}$ Mpc for the galaxies brighter than $M = -20.5$. For the brightest galaxies in the sample with $M \leq -21$ the correlation length reaches values as high as $\sim 16 h^{-1}$ Mpc. These galaxies are not preferentially found in rich clusters and the study of their properties will be the subject of a separate paper. The relative bias is scale independent up to $\sim 13 h^{-1}$ Mpc and the linear bias between the brightest and L_* galaxies is in the range 1.5-2.

A preliminary comparison with presently available models of galaxy formation shows serious difficulties in modeling simultaneously the faint and bright ends of the bias variation with luminosity evidenced in the SSRS2. However, more data is necessary to allow a better determination of the behavior of luminosity biasing at faint luminosities which is strongly affected by sampling variations for nearby catalogs, although it is constrained to be small by our analysis. On the theoretical side, a better understanding galaxy formation and of the galaxy-dark-halo connection is required in order to use these results as useful constraints to galaxy formation models.

We would like to thank all the SSRS2 collaborators for allowing us to use the data in advance of its publication. We are grateful to George Efstathiou, Guinevere Kauffmann, Amos Yahil and Simon White for fruitful discussions. LNdC would like to thank the hospitality of the IAP and of the DAEC where most of the work was carried out. We would like to thank the referee, Jo Ann Eder, for her constructive comments.

REFERENCES

- Alimi, J-M., Valls-Gabaud, D. & Blanchard, A., 1988, *A&A*, 206, L11
- Bardeen, J.M., Bond, J.R., Kaiser, N. & Szalay, A.S., 1986, *ApJ*, 304, 15
- Balian, R. & Schaeffer, R., 1989, *A&A*, 220, 1
- Baryshev, Y.V., Sylos Labini, F., Montuori, M., & Pietronero, L., 1994, *Vistas in Astronomy*, 38, 419
- Bernardeau, F., & Schaeffer, R., 1992, *A&A*, 255, 1
- Bingelli, B., Tarenghi, M., & Sandage, A., 1990, *A&A*, 228, 42
- Börner, G., Mo, H.J. & Zhou, 1989, *A&A*, 221, 191
- Börner, G., Deng, Z.G., & Xia, X.Y., 1989, *A&A*, 209, 1
- Börner, G., & Mo, H.J., 1990, *A&A*, 227, 324
- Cappi, A., da Costa, N.L., Benoist, C. & Maurogordato, S., in preparation
- da Costa, N.L., Pellegrini, P.S., Sargent, W.L.W., Tonry, J., Davis, M., Meiskin, A., Latham, D.W., Menzies, J.W. & Coulson, J.A., 1988, *ApJ*, 327, 544
- da Costa, N.L., Geller, M.J., Pellegrini, P.S., Latham, D.W., Fairall, A.P., Marzke, R.O., Willmer, C.N.A., Huchra, J.P., Calderon, J.H., Ramella, M. & Kurtz, M.J., 1994, *ApJ Letters*, 424, L1
- da Costa, L.N., Vogeley, M., Geller, M.J., Huchra, J., & Park, C., 1994, *ApJ*, 437, L1
- Davis, M., & Geller, M.J., 1976, *ApJ*, 208, 13
- Davis, M., & Peebles, P.J.E., 1983, *ApJ*, 267, 465

- Davis, M., Meiksin, A., Strauss, M.A., da Costa, N.L., & Yahil, A., 1988, ApJ, 333, L9
- Dominguez-Tenreiro, R., & Martinez, V.J., 1989, ApJ, 339, L9
- Dominguez-Tenreiro, R., Campos, A., Gómez-Flechoso, M.A., & Yepes, G., 1994, ApJ, 424, L73
- Eder, J.A., Schombert, J.M., Dekel, A., & Oemler, A., 1989, ApJ, 340, 29
- Efstathiou, G., Ellis, R.S. & Peterson, B.A., 1988, MNRAS, 232, 43
- Hamilton, A.J.S., 1988, ApJ, 331, L59
- Hamilton, A.J.S., 1993, ApJ, 417, 19
- Hasegawa, T., & Umemura, M., 1993, MNRAS, 263, 191
- Haynes, M.P., & Giovanelli, R., 1989, in Large Scale Motion of the Universe, ed. Rubin & Coyne (Princeton U.P.), 31
- Huchra, J., Davis, M., Latham, D., & Jonry, J., 1983, ApJS, 52, 89
- Iovino, A., Giovanelli, R., Haynes, M., Chicarini, G., & Guzzo, L., 1993, MNRAS, 265, 21
- Kaiser, N., 1987, MNRAS, 227, 1
- Kauffmann, G., 1995, private communication
- Lachièze-Rey, M., da Costa, N.L., & Maurogordato, S., 1992, ApJ, 399, 10
- Loveday, J., Maddox, S.J., Efstathiou, G., & Peterson, B.A., 1995, ApJ, 442, 457
- Marzke, R.O., Geller, M.J., da Costa, L.N., & Huchra, J.P., 1994, CFA preprint
- Maurogordato, S., & Lachièze-Rey, M., 1991, ApJ, 369, 30

- Maurogordato, S., Schaeffer, R., & da Costa, L.N., 1992, ApJ, 390, 17
- Mo, H.J., Einasto, M., Xia, X.Y., & Deng, Z.G., 1992, MNRAS, 255, 382
- Mo, H.J., & White, S.D.M., 1995, MNRAS, submitted
- Park, C., Vogeley, M.S., Geller, M.J., & Huchra, J.P., 1994, ApJ, 431, 569
- Peebles, P.J.E., 1980, The Large Scale Structure of the Universe (Princeton: Princeton Univ. Press)
- Phillipps, S., & Shanks, T., 1987, MNRAS, 229, 621
- Santiago, B.X., & da Costa, N.L., 1990, ApJ, 362, 386
- Schaeffer, R., 1984, A&A, 134, L15
- Schaeffer, R., 1985, A&A, 144, L1
- Schaeffer, R., 1987, A&A, 180, L5
- Thuan, T.X., Gott III, J.R., & Schneider, S.E., 1987, ApJ, 315, L93
- Thuan, T.X., Alimi, J.M., Gott, J.R., & Schneider, S.E., 1991, ApJ, 370, 25
- Valls-Gabaud, D., Alimi, J.M., & Blanchard, A., 1989, Nature, 341, 215
- White, S.D.M., Davis, M., Efstathiou, G., & Frenk, C.S., 1987, Nature, 330, 351
- White, S.D.M., Tully, R.B., & Davis, M., 1988, ApJ, 333, L45
- Yahil, A., Tammann, G.A., & Sandage A., 1977, ApJ, 217, 903

Fig. 1.— The two-point correlation function in redshift space $\xi(s)$ (panel a), the $J_3(s)$ integral (panel b) and the variance $\sigma^2(s)$ (panel c) calculated from counts in cells for SSRS2 volume-limited subsamples identified as follows : D30 (stars); D38 (full triangles); D48 (opened triangles); D60 (full pentagons); D74 (opened pentagons); D91 (full squares); D112 (open squares); D138 (full circles); D168 (open circles).

Fig. 2.— The variation of $\xi(s)$ with luminosity is tested within subsamples at a given depth. In each panel, we present $\xi(s)$ for two luminosity classes of one magnitude range within the same volume. In panel a), galaxies with $-18.5 < M < -17.5$ and $-19.5 < M < -18.5$ are compared within a volume of $38h^{-1}Mpc$ depth. In panel b), galaxies with $-19.5 < M < -18.5$ and $-20.5 < M < -19.5$ are compared within a volume of $60h^{-1}Mpc$ depth. In panel c), galaxies with $-20.5 < M < -19.5$ and $-21.5 < M < -20.5$ are compared within a volume of $91h^{-1}Mpc$ depth.

Fig. 3.— The redshift space correlation function $\xi(s)$ is displayed in various panels, each corresponding to a given luminosity class: $-19.5 < M < -18.5$ in panel a), $-20.5 < M < -19.5$ in panel b), $-21.5 < M < -20.5$ in panel c). Within each panel, $\xi(s)$ is presented for three different volumes. Symbols vary from opened triangles to opened squares and full squares with increasing size of the sample.

Fig. 4.— The biasing factor as a function of separation, for subsamples D74 to D168. It is normalized to the value b^* calculated from sample D91 corresponding to galaxies brighter than L^* . In panel a), the biasing factor is derived from J_3 , and in panel b) from σ^2 .

Fig. 5.— Evolution of b/b^* (averaged between $2h^{-1}Mpc$ and $13h^{-1}Mpc$) with the limiting absolute magnitude of the sample . Our results from SSRS2 are reported as full squares when derived from J_3 , and as open squares when derived from σ^2 . CfA results of Hamilton (1988) are shown as opened triangles. Results from CDM simulations of White et al. (1987)

as given by Valls-Gabaud et al. (1989) are plotted as a long-dashed line. On this graph are over-plotted analytical predictions by Mo and White (1995), with low ($\sigma_8 = 0.5$, dotted line) and high normalizations ($\sigma_8 = 1$, short-dashedline) and by Bernardeau & Schaeffer (1992) (dashed-dotted line).

Table 1. Subsamples of the SSRS2.

Sample	D ($h^{-1}\text{Mpc}$)	M_{lim}	N_g	\bar{n} ($10^{-3}h^3\text{Mpc}^{-3}$)	s_0 ($h^{-1}\text{Mpc}$)	γ	s_0t ($h^{-1}\text{Mpc}$)	Interval ($h^{-1}\text{Mpc}$)	σ_8^2	L/E
D30	30.69	-17.0	301	27.2	4.3 ± 0.5	1.7 ± 0.2	4.3 ± 0.4	2.0-5.2	-	2.3
D38	38.35	-17.5	329	15.5	4.5 ± 0.4	1.6 ± 0.2	4.4 ± 0.3	2.0-5.2	-	2.2
D48	47.83	-18.0	487	11.8	3.5 ± 0.2	2.1 ± 0.2	3.5 ± 0.2	2.0-5.0	0.3	2.2
D60	59.52	-18.5	774	9.7	4.8 ± 0.5	1.3 ± 0.1	4.6 ± 0.3	2.0-8.0	0.5	2.0
D74	73.86	-19.0	770	5.1	5.5 ± 0.4	1.4 ± 0.1	5.2 ± 0.4	2.0-8.0	0.7	1.9
D91	91.37	-19.5	755	2.6	5.8 ± 0.6	1.7 ± 0.2	5.8 ± 0.4	2.0-12.6	0.9	2.1
D112	112.60	-20.0	593	1.1	5.5 ± 0.6	2.0 ± 0.3	5.5 ± 0.4	2.0-12.6	0.9	2.2
D138	138.12	-20.5	268	0.3	8.0 ± 0.4	2.0 ± 0.2	8.5 ± 0.5	2.0-15.8	1.5	2.5
D168	168.52	-21.0	133	0.1	15.8 ± 2.9	1.5 ± 0.3	15.2 ± 2.0	2.5-25.0	3.0	1.7

Table 2. Characteristics of subsamples in magnitude bins.

Sample	D ($h^{-1}\text{Mpc}$)	N_g
-18.5/-17.5	38.35	187
-19.5/-18.5	38.35	105
-19.5/-18.5	47.83	227
-19.5/-18.5	59.52	563
-20.5/-19.5	59.52	193
-20.5/-19.5	73.86	329
-20.5/-19.5	91.37	687
-21.5/-20.5	91.37	67
-21.5/-20.5	112.60	155
-21.5/-20.5	138.12	268

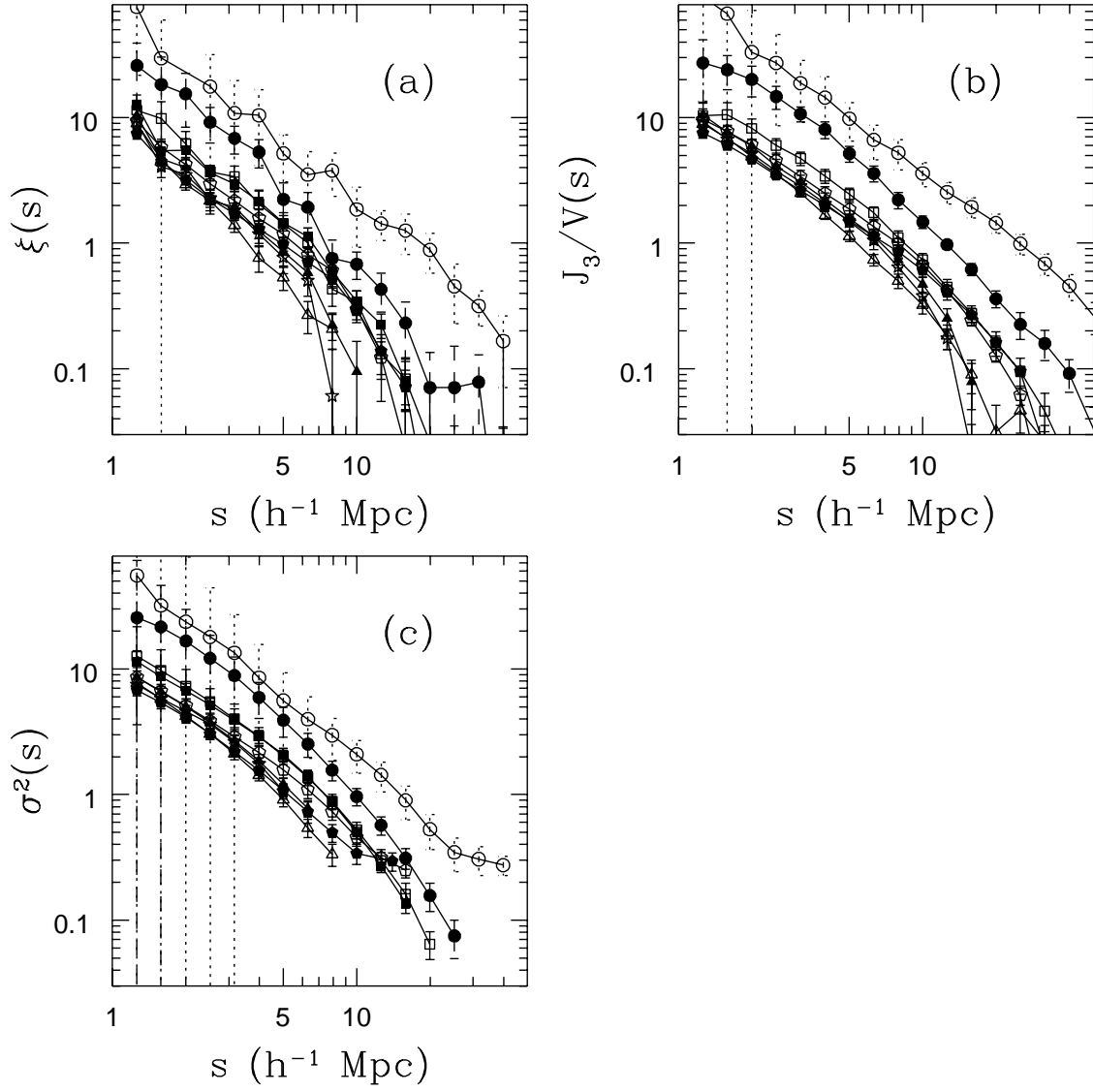


Fig. 1.—

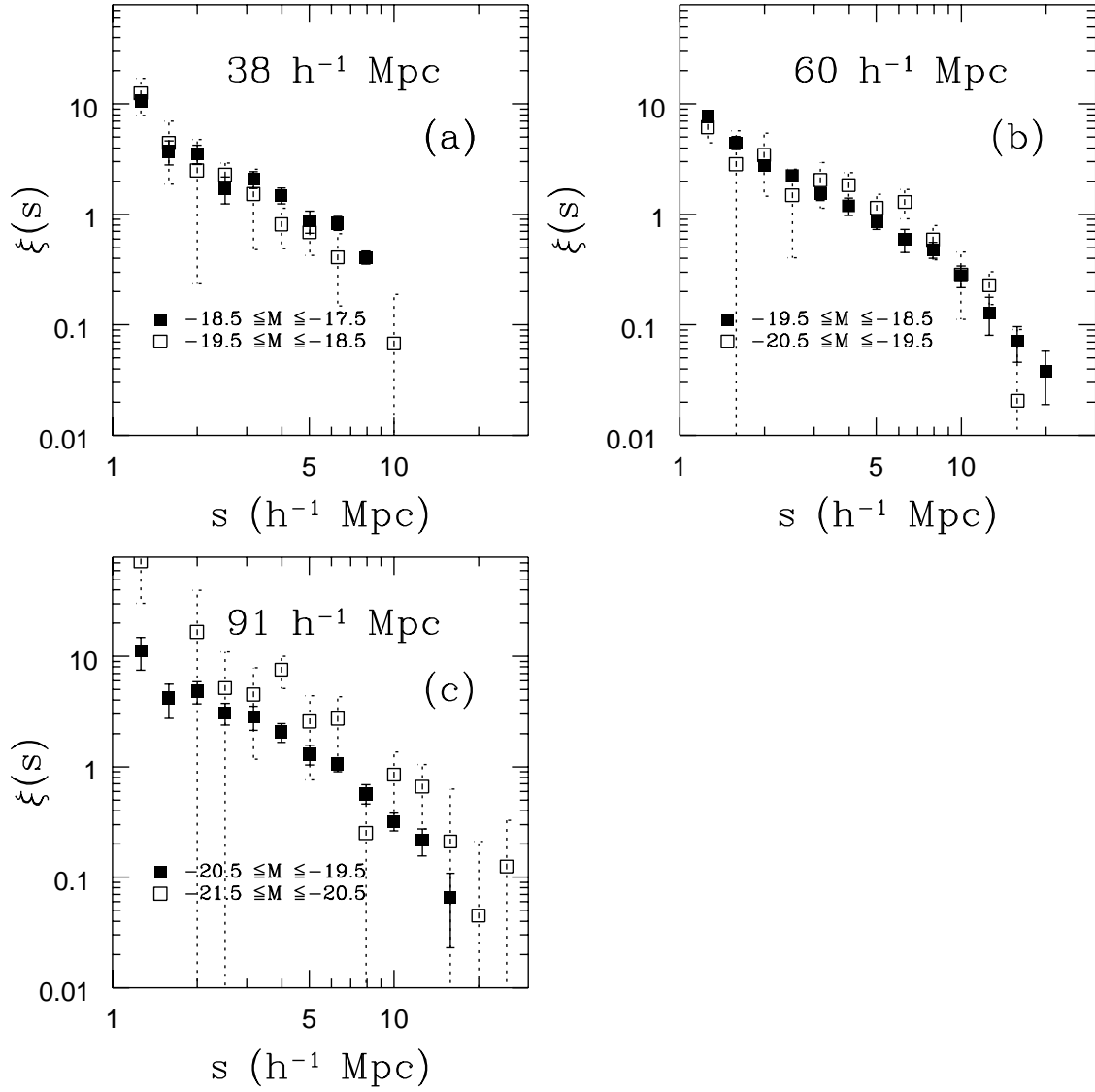


Fig. 2.—

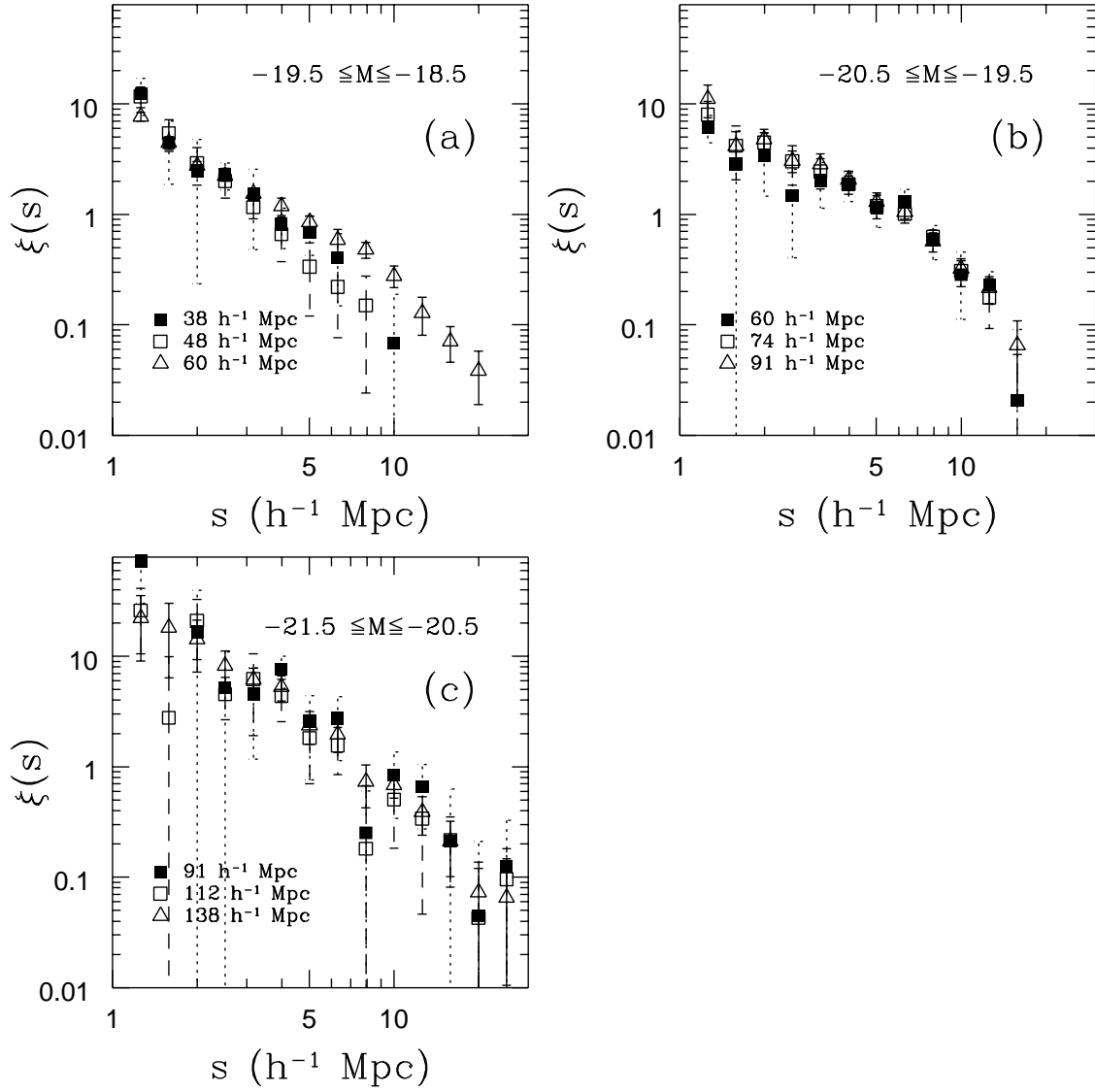


Fig. 3.—

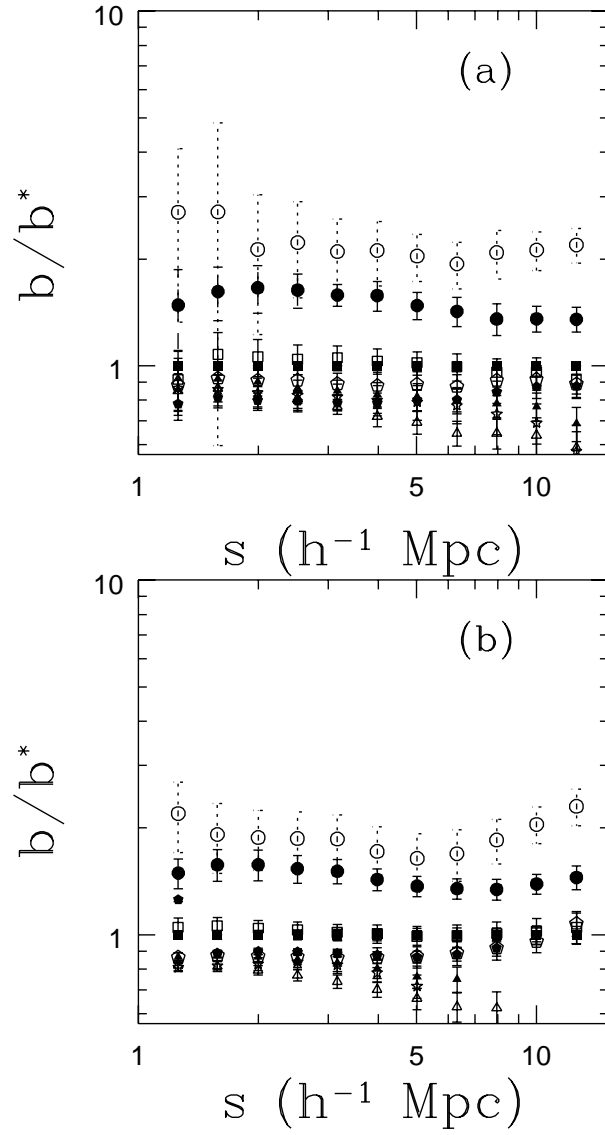


Fig. 4.—

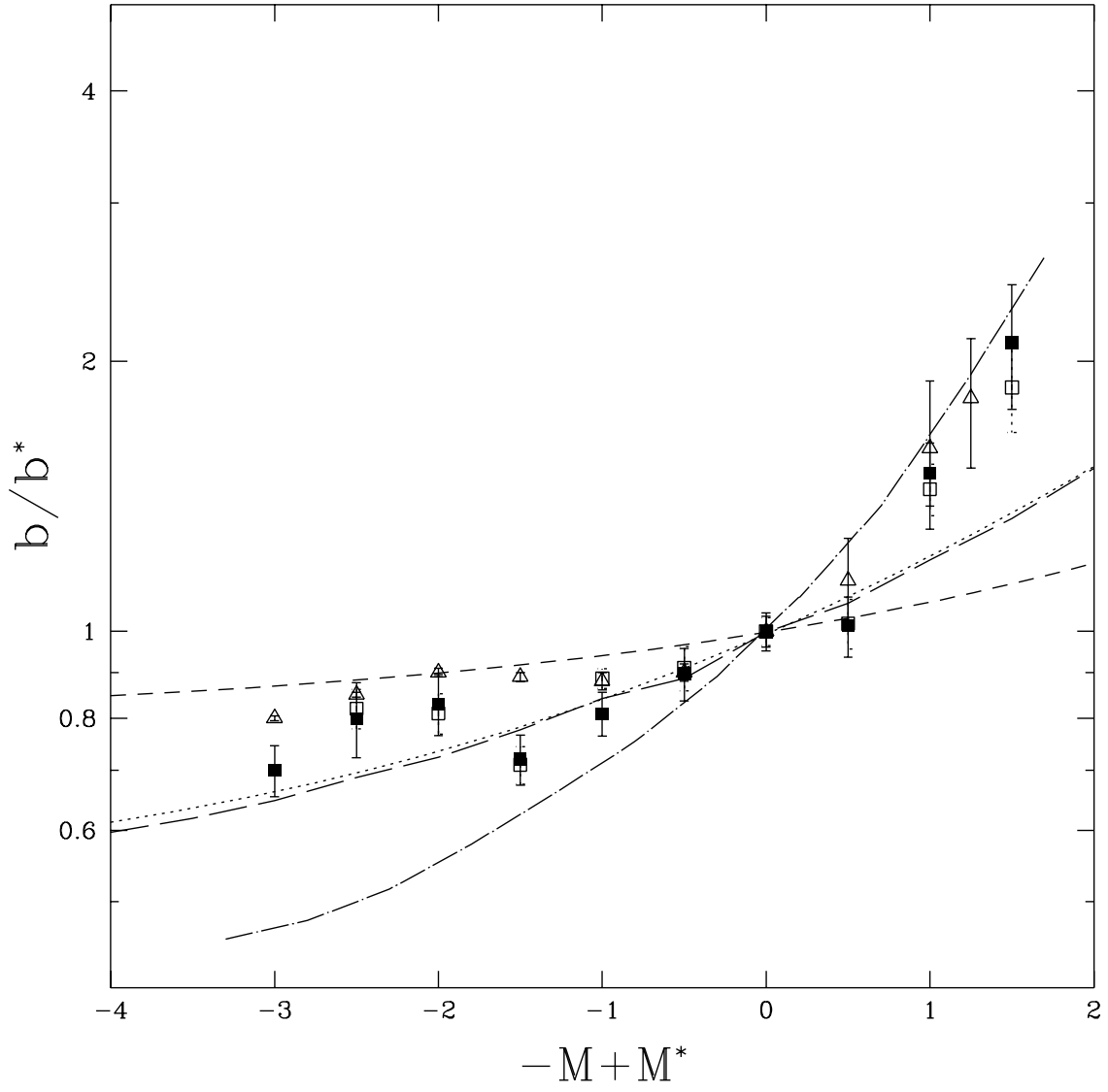


Fig. 5.—